



133  
019  
THS

PHOTOELASTIC CONSTANTS OF SYNTHETIC SAPPHIRE

Thesis for the Degree of M. S.

MICHIGAN STATE UNIVERSITY

David L. Bradley

1963

THESIS  
C.2



**PLACE IN RETURN BOX**  
to remove this checkout from your record.  
**TO AVOID FINES** return on or before date due.

DATE DUE	DATE DUE	DATE DUE

PHOTOELASTIC CONSTANTS OF SYNTHETIC SAPPHIRE

BY

David L. Bradley

AN ABSTRACT OF A THESIS

Submitted to  
Michigan State University  
in partial fulfillment of the requirements  
for the degree of

MASTER OF SCIENCE

Department of Physics and Astronomy

1963

David L. Bradley

ABSTRACT

The photoelastic constants of synthetic sapphire were determined by combining both static and dynamic measurements. Procedures for obtaining photoelastic constants in rotated coordinate systems, corresponding to specific orientations of the sapphire crystals are outlined. The ratios of photoelastic constants are measured by analyzing the polarization of the first order diffraction pattern produced by pure longitudinal ultrasonic waves. The differences of photoelastic constants are obtained by applying a known stress to the sample and measuring the phase difference of the light with a Babinet Compensator. Values of the strain optical and stress optical constants are tabulated.

PHOTOELASTIC CONSTANTS OF SYNTHETIC SAPPHIRE

BY

David L. Bradley

A THESIS

Submitted to  
Michigan State University  
in partial fulfillment of the requirements  
for the degree of

MASTER OF SCIENCE

Department of Physics and Astronomy

1963

11526  
2/20/61  
H. L. B.

#### ACKNOWLEDGMENTS

The author wishes to extend thanks to Dr. E. A. Hiedemann for suggesting this investigation and for his interest during its execution. The assistance of Dr. W. G. Mayer and Dr. K. Achyuthan is also greatly appreciated. The time and effort of Mr. Verne Hulce was an invaluable aid.

D. L. B.

## TABLE OF CONTENTS

	Page
INTRODUCTION.....	1
THEORY.....	4
EXPERIMENTAL PROCEDURE.....	21
EXPERIMENTAL RESULTS.....	27
REFERENCES.....	33



## LIST OF TABLES

Table	Page
I. Directions of sound propagation, directions of observation, and corresponding ratios of photoelastic constants.....	19, 20
II. Tabulation of strain optical constants.....	32
III. Tabulation of stress optical constants.....	32

## LIST OF FIGURES

Figure	Page
1. Directions of pure longitudinal motion in the X-Y plane.....	5
2. Directions of pure longitudinal motion in the Y-Z plane.....	5
3. Rotation of the sapphire sample about the X-axis.....	5
4. Diagram of the optical arrangement for the dynamic measurements.....	22
5. Diagram of the optical arrangement for the static measurements.....	25
6. Illustrations of the static stressing bench.....	26
7. Experimental data for ratios of photoelastic constants.....	29
8. Experimental data for ratios of photoelastic constants.....	30

## INTRODUCTION

Photoelasticity, the phenomenon of double refraction accompanying mechanical stress, was discovered in 1815 by Sir David Brewster. Early work in this field was carried out by F. E. Neumann, who was the first investigator to systematically develop a theory of double refraction due to a stress. G. Wertheim was the first to experimentally verify the laws of photoelasticity for homogeneous stresses in glasses (1).

Other investigators contributing to the early work in this field were J. Kerr, who experimentally found the first reliable values for the stress-optical constants, and C. Maxwell, who proposed essentially the same theory as F. E. Neumann.

In 1889 and 1890, the elementary theory of double refraction was extended to crystals by F. Pockels (1).

Early investigators were limited in their measurements of photoelastic constants to static measurements. A relative change in the optical path length could be measured by applying a stress in a given direction and measuring the difference in optical path length with a Babinet Compensator for light polarized normal to the stress direction and light polarized parallel to the stress direction. The difference in optical path length is proportional to the difference of photoelastic constants. Absolute changes in optical path length were measured using interferometric

techniques. An absolute change in optical path length is proportional to the photoelastic constant for that direction.

In 1932, the discovery of the effect of an ultrasonic field on light passing through a transparent material led to an entirely new method of determining photoelastic constants. H. Mueller, (2), (3), (4), developed a theory of the diffraction of light by ultrasound in isotropic solids. Mueller's theory is an adaptation of the theory of the diffraction of light by ultrasound in liquids by Raman and Nath (5). Mueller's theory was experimentally verified by Hiedemann. Narasimhamurty (6) investigated the photoelastic constants of uniaxial and biaxial crystals, following the suggestions of Mueller. Photoelastic constants of isotropic solids and crystals may be studied using static methods first developed and using dynamic methods, suggested by Mueller (2).

In this investigation, static and dynamic measurements were both employed to determine the photoelastic constants of synthetic sapphire. The photoelastic constants may be divided into two classes, the stress-optical constants and the strain-optical constants, the former related to variations of stress and the latter related to variation of strain. In this dissertation, we shall assume stress and strain to be within the limits of Hooke's Law. In this case, the two systems may be used equivalently. We shall also assume stress and strain to lie along the same axis,

i. e., a pure compressional force.

Sapphire belongs to the trigonal class of crystals.

It is a negative uniaxial ( the ordinary index of refraction is greater than the extraordinary index of refraction) crystal with eight stress optical (or strain optical) constants.

Investigations were performed on three samples of sapphire oriented at particular angles with respect to an orthogonal set of axes. Three samples were necessary to provide enough relationships to obtain the eight constants of sapphire. The static measurements were performed in the usual way, using a Babinet Compensator to measure the relative change in the optical path. The dynamic measurements were made using Mueller's Method "C", described in the experimental section.

Photoelastic constants describe the optical behavior of sapphire when subjected to stress or strain. Knowledge of the photoelastic constants, when coupled with the intensity distribution of light in the diffraction orders created by a sound field, provide a method of studying absolute sound pressure amplitude.

## THEORY

SECTION A: The assumption of pure longitudinal waves in this investigation demands a determination of the directions in a trigonal crystal along which these pure longitudinal waves can be propagated. F. E. Borgnis (7) has developed a general theory for determining the directions of pure longitudinal waves in crystals.

In general, the particle displacement in a crystal does not coincide with that of the pressure wave. There are, however, certain crystallographic orientations for which the direction of particle displacement and the direction of pressure wave propagation coincide. Following Borgnis, a set of relationships between the direction cosines ( $\ell_i$ ) of the pure longitudinal waves and an orthogonal set of axes are obtained:

$$\ell_1 = 1, \quad \ell_2 = \ell_3 = 0 \quad (1)$$

$$\ell_3 = 1, \quad \ell_1 = \ell_2 = 0 \quad (2)$$

$$(-c_{13} + c_{33} - 2 c_{44}) \left( \frac{\ell_3}{\ell_2} \right)^3 + 3 c_{14} \left( \frac{\ell_3}{\ell_2} \right)^2 + (-c_{11} + c_{13} + 2 c_{44}) \ell_1$$

$$\left( \frac{\ell_3}{\ell_2} \right) - c_{14} = 0 \quad (3)$$

$$\ell_1 = 0$$

From Eq. (1), pure longitudinal waves may exist along the X-axis of the crystal. For a trigonal system, a rotation of  $120^\circ$  about the Z-axis produces an equivalent coordinate system. Figure 1 indicates the directions of pure longitudinal waves in the X-Y plane.

**FIG.1. LONGITUDINAL  
MOTION IN X-Y PLANE**

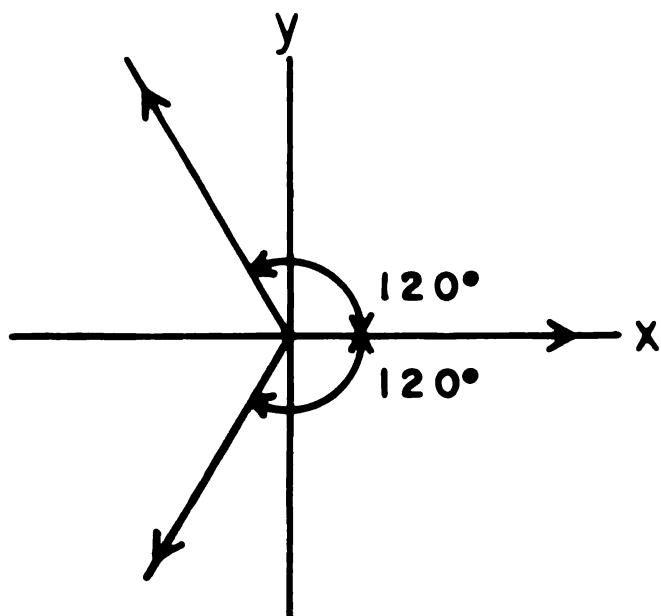


**FIG.2. LONGITUDINAL  
MOTION IN Y-Z PLANE**

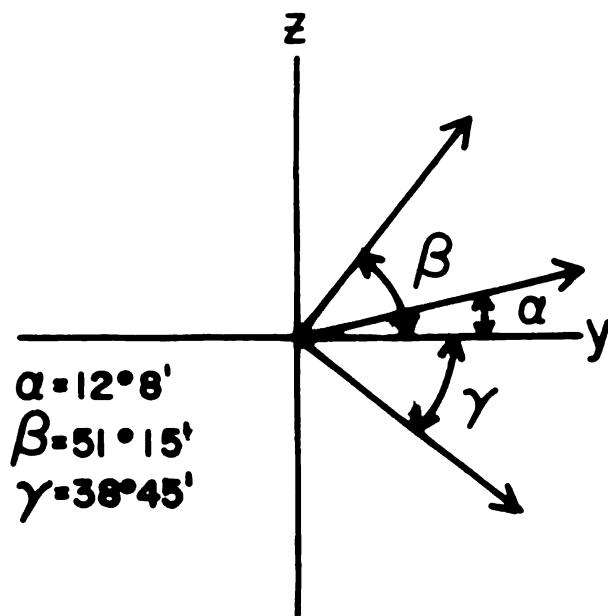
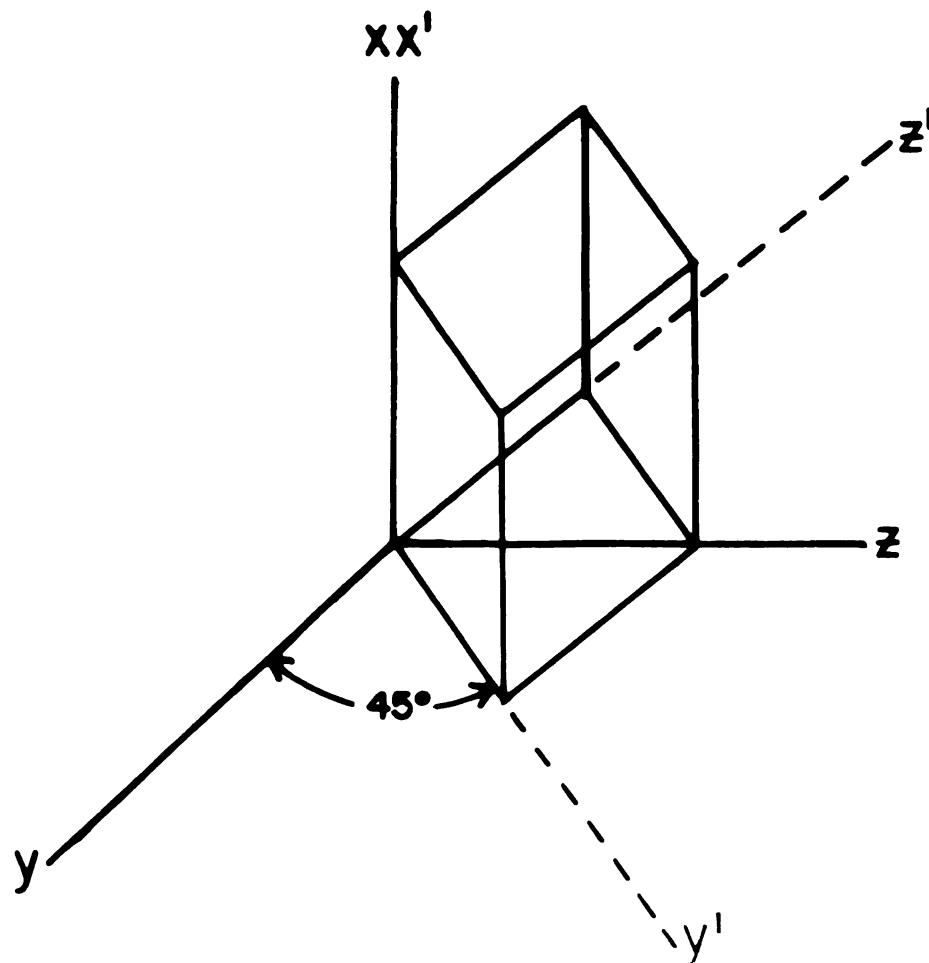


**FIG.3. ROTATED SAMPLE; SOUND ALONG  $X'$ -AXIS; LIGHT,  $Y'$ -AXIS**



From Eq. (2), pure longitudinal waves can be propagated along the Z-axis of the crystal. Equation (3) gives a set of directions in the Y-Z plane along which pure longitudinal waves may exist. Substituting the values of elastic constants as given by Mayer and Hiedemann (8) into Eq. (3) and solving for  $\frac{\ell_3}{\ell_2}$  one obtains the following three sets of values for  $\ell_2$  and  $\ell_3$ :

$$\begin{array}{lll} \ell_2 = + .620 & \ell_2 = + .775 & \ell_2 = .978 \\ \ell_3 = + .784 & \ell_3 = - .632 & \ell_3 = .210 \end{array}$$

Figure 2 illustrates the orientation of these angles with respect to the Y-axis and Z-axis. Counting positive and negative directions, there are thirteen possible directions of pure longitudinal motion.

SECTION B: F. Pockels (1), (9) developed a systematic method of studying the photoelastic constants of crystals. His argument is as follows; Assuming that Fresnel's laws of propagation of light hold in a crystalline medium, the optical index ellipsoid in an undeformed medium may be represented in general by:

$$B_{11}^0 x^2 + B_{22}^0 y^2 + B_{33}^0 z^2 + 2 B_{23}^0 yz + 2 B_{31}^0 zx + 2 B_{12}^0 xy = 1 \quad (4)$$

where

$$B_{11}^0 = \frac{1}{n_{11}^2}, \dots, B_{12}^0 = \frac{1}{n_{12}^2}.$$

In a deformed medium, the optical index ellipsoid is, in general

$$B_{11} x^2 + B_{22} y^2 + B_{33} z^2 + 2 B_{23} yz + 2 B_{31} zx + 2 B_{12} xy = 1 \quad (5)$$



$$\text{where } B_{11} = \frac{1}{n_{11}'^2}, \dots, B_{12} = \frac{1}{n_{12}'^2}$$

The  $n_{ij}$  and  $n_{ij}'$  may be called the optical parameters of the system. Pockels assumed that the differences of the corresponding coefficients of the two index ellipsoids can be expressed as a linear function of the strain, i.e.,

$$B_{11} - B_{11}^0 = p_{11}S_{11} + p_{12}S_{22} + p_{13}S_{33} + p_{14}S_{23} + p_{15}S_{31} + p_{16}S_{12} \quad (6)$$

$$B_{12} - B_{12}^0 = p_{61}S_{11} + p_{62}S_{22} + p_{63}S_{33} + p_{64}S_{23} + p_{65}S_{31} + p_{66}S_{12}$$

where the  $p_{ij}$  are the strain-optical constants and the  $S_{mn}$  are the components of strain. Since the investigation is conducted in the region where Hooke's law holds, stress may be substituted for strain to give the following set of equations:

$$B_{11} - B_{12}^0 = -(q_{11}T_{11} + q_{12}T_{22} + q_{13}T_{33} + q_{14}T_{23} + q_{15}T_{31} + q_{16}T_{12}) \quad (7)$$

$$B_{12} - B_{12}^0 = -(q_{61}T_{11} + q_{62}T_{22} + q_{63}T_{33} + q_{64}T_{23} + q_{65}T_{31} + q_{66}T_{12})$$

where the  $q_{ij}$  and  $T_{mn}$  are the stress-optical constants and the components of stress respectively. The  $p_{ij}$  and  $q_{ij}$  compose the photoelastic constants of a crystal. The components of stress and strain are related by elastic constants and moduli as follows:

$$-S_{11} = s_{11}T_{11} + s_{12}T_{22} + s_{13}T_{33} + s_{14}T_{23} + s_{15}T_{31} + s_{16}T_{12} \quad (8)$$

$$-S_{12} = s_{61}T_{11} + s_{62}T_{22} + s_{63}T_{33} + s_{64}T_{23} + s_{65}T_{31} + s_{66}T_{12}$$

where the  $s_{ij}$  are the elastic moduli.



$$-T_{11} = c_{11}S_{11} + c_{12}S_{22} + c_{13}S_{33} + c_{14}S_{23} + c_{15}S_{31} + c_{16}S_{12} \quad (9)$$

$$-T_{12} = c_{61}S_{11} + c_{62}S_{22} + c_{63}S_{33} + c_{64}S_{23} + c_{65}S_{31} + c_{66}S_{12}$$

where the  $c_{ij}$  are the elastic constants. Combining Eqs. (6), (7), (8), and (9), one obtains:

$$p_{k1} = \sum_{j=1}^6 q_{kj} c_{j1} \quad q_{k1} = \sum_{j=1}^6 p_{kj} s_{j1} \quad (10)$$

where the indices  $k, l = 1, \dots, 6$  also.

In order to avoid repetition, only the  $p_{ij}$  will be discussed henceforth, but the assumption of working in the region where Hooke's law is valid makes it possible to use the relationships derived for the  $q_{ij}$  also.

In the most general case, there would be 36 different constants  $p_{ij}$  for the triclinic crystal. Crystal symmetry reduces the number of constants to eight in the case of sapphire, which is a trigonal crystal. Pockels' equations may be written in matrix form for the trigonal system as follows:

$$\begin{array}{l} B_{11} - B_{11}^0 = \\ B_{22} - B_{22}^0 = \\ B_{33} - B_{33}^0 = \\ B_{23} - B_{23}^0 = \\ B_{31} - B_{31}^0 = \\ B_{12} - B_{12}^0 = \end{array} \begin{bmatrix} p_{11} & p_{12} & p_{13} & p_{14} & 0 & 0 \\ p_{12} & p_{11} & p_{13} & -p_{14} & 0 & 0 \\ p_{31} & p_{31} & p_{33} & 0 & 0 & 0 \\ p_{41} & -p_{41} & 0 & p_{44} & 0 & 0 \\ 0 & 0 & 0 & 0 & p_{44} & 2p_{41} \\ 0 & 0 & 0 & 0 & p_{14} & p_{11} - p_{12} \end{bmatrix} \begin{bmatrix} S_{11} \\ S_{22} \\ S_{33} \\ S_{23} \\ S_{31} \\ S_{12} \end{bmatrix} \quad (11)$$



It is this set of constants that is to be investigated.

Consider two illustrative cases of calculating photoelastic constants.

Case 1: The crystal is oriented along the orthogonal set (X-Y-Z) of axes. Strain is along the Z-axis and observation along the Y-axis. With no strain, the cross section of the undisturbed index ellipsoid is represented by:

$$B_{11}^0 x^2 + B_{33}^0 z^2 = 1 \quad (12)$$

Upon application of a strain, the index ellipsoid is distorted and the ellipsoid cross section is represented by:

$$B_{11} x^2 + B_{33} z^2 + 2B_{31} zx = 1 \quad (13)$$

where the  $B_{31}$  term indicates the ellipse is, in general, tilted with respect to the orthogonal axes. From Eq. (11), one obtains:

$$\begin{aligned} B_{11} - B_{11}^0 &= p_{11}S_{11} + p_{12}S_{22} + p_{13}S_{33} + p_{14}S_{23} \\ B_{33} - B_{33}^0 &= p_{31}S_{11} + p_{32}S_{22} + p_{33}S_{33} \\ B_{31} - B_{31}^0 &= p_{41}S_{31} + 2p_{41}S_{12} \end{aligned} \quad (14)$$

where  $B_{31}^0 = 0$ , since the index ellipse is not tilted in the absence of strain. Since the only strain is along the Z-axis, all the  $S_{mn}$  are zero except  $S_{33}$ . Eq. (14) can then be written as:

$$\begin{aligned} B_{11} - B_{11}^0 &= p_{13}S_{33} \\ B_{33} - B_{33}^0 &= p_{33}S_{33} \\ B_{31} &= 0, \end{aligned} \quad (15)$$

Indicating in this particular case that the cross section of the index ellipsoid is not tilted with respect to the X-Z axes.

1. The first part of the document discusses the importance of maintaining accurate records of all transactions and activities. It emphasizes that proper record-keeping is essential for transparency and accountability, particularly in financial matters. The text suggests that organizations should implement robust systems to track every aspect of their operations, from procurement to sales.

2. In the second section, the author addresses the challenges of data management in a rapidly changing environment. It highlights the need for flexible and scalable solutions that can adapt to new technologies and evolving business requirements. The text also touches upon the importance of data security and privacy, noting that organizations must take appropriate measures to protect sensitive information from unauthorized access and breaches.

3. The third part of the document focuses on the role of technology in enhancing operational efficiency. It explores various digital tools and platforms that can streamline processes, reduce errors, and improve overall productivity. The author argues that embracing technology is not just a choice but a necessity for organizations looking to stay competitive in the modern market.

4. The fourth section discusses the importance of continuous learning and development for the workforce. It suggests that organizations should invest in training programs and provide opportunities for employees to acquire new skills and knowledge. This not only helps in keeping the workforce up-to-date with the latest industry trends but also fosters a culture of innovation and growth within the organization.

5. Finally, the document concludes by emphasizing the need for strong leadership and strategic vision. It states that effective leaders are those who can inspire their teams, set clear goals, and navigate the organization through complex challenges. The text encourages leaders to remain adaptable and open to change, as these qualities are crucial for long-term success in a dynamic business landscape.

Case 2: The crystal is oriented at an angle with respect to the orthogonal (X-Y-Z) set of axes. For this example, assume the crystal has been rotated  $45^\circ$  about the X-axis. The strain is along the X'-axis and observation is along the Y'-axis and indicated in Fig. 3. The rotation matrix may be written as follows:

$$\begin{array}{ccc|ccc}
 & & & x' & y' & z' \\
 & & & \hline
 x & \ell_1 & m_1 & n_1 & & \\
 y & \ell_2 & m_2 & n_2 & & \\
 z & \ell_3 & m_3 & n_3 & & 
 \end{array} \quad (16)$$

where the  $\ell_i$ ,  $m_i$ , and  $n_i$  are direction cosines relating the X', Y', Z' axes with the original X, Y, Z axes. For a specific rotation of  $45^\circ$  about the X-axis, Eq. (16) becomes

$$\begin{array}{ccc|ccc}
 & & & x' & y' & z' \\
 & & & \hline
 x & 1 & 0 & 0 & & \\
 y & 0 & 1/\sqrt{2} & -1/\sqrt{2} & & \\
 z & 0 & 1/\sqrt{2} & 1/\sqrt{2} & & 
 \end{array} \quad (17)$$

Using Eq. (16) and rewriting the strain of the original coordinate system in terms of the strains in the new coordinate system, one obtains

$$\begin{aligned}
 s_{11} &= s'_{11}\ell_1^2 + s'_{22}m_1^2 + s'_{33}n_1^2 + 2(s'_{23}m_1n_1 + s'_{31}n_1\ell_1 + s'_{12}\ell_1m_1) \\
 \hline
 s_{12} &= s'_{11}\ell_1\ell_2 + s'_{22}m_1m_2 + s'_{33}n_1n_2 + s'_{23}(m_1n_2 + m_2n_1) + s'_{31}(n_1\ell_2 + \ell_1n_2) \\
 &\quad + s'_{12}(\ell_1m_2 + \ell_2m_1)
 \end{aligned} \quad (18)$$

where  $S'_{mn}$  are the strains in the new system. Using Eq. (17), one may write;

$$\begin{aligned}
 S_{11} &= S'_{11} & S_{23} &= \frac{1}{2} S'_{22} - \frac{1}{2} S'_{33} \\
 S_{22} &= \frac{1}{2} S'_{22} + \frac{1}{2} S'_{33} - S'_{23} & S_{31} &= \frac{1}{\sqrt{2}} S'_{31} + \frac{1}{\sqrt{2}} S'_{12} \\
 S_{33} &= \frac{1}{2} S'_{22} + \frac{1}{2} S'_{33} + S'_{23} & S_{12} &= \frac{1}{\sqrt{2}} S'_{31} + \frac{1}{\sqrt{2}} S'_{12}
 \end{aligned} \quad (19)$$

Now the equation for the differences of coefficients of the index ellipsoid may be written in terms of the strains in the new system.

Combining Eqs. (11) and (19),

$$\begin{aligned}
 B_{11} - B_{11}^0 &= p_{11} S'_{11} + \frac{1}{2} (p_{12} + p_{13} + p_{14}) S'_{22} + \frac{1}{2} (p_{12} + p_{13} - p_{14}) S'_{33} \\
 &\quad + (-p_{12} + p_{13}) S'_{23} \\
 B_{12} - B_{12}^0 &= \frac{1}{\sqrt{2}} (p_{41} - p_{11} + p_{12}) S'_{31} + \frac{1}{\sqrt{2}} (p_{41} + p_{11} - p_{12}) S'_{12}
 \end{aligned} \quad (20)$$

Since only a strain along the  $X'$ -axis is being considered, the  $S'_{mn}$  are all zero, except  $S'_{11}$ . Therefore, Eq. (20) reduces to:

$$\begin{aligned}
 B_{11} - B_{11}^0 &= p_{11} S'_{11} & B_{23} - B_{23}^0 &= p_{41} S'_{11} \\
 B_{22} - B_{22}^0 &= p_{12} S'_{11} & B_{31} - B_{31}^0 &= 0 \\
 B_{33} - B_{33}^0 &= p_{31} S'_{11} & B_{12} - B_{12}^0 &= 0
 \end{aligned} \quad (21)$$

Now consider the index ellipsoid in the rotated system:

$$A_{11} x'^2 + A_{22} y'^2 + A_{33} z'^2 + 2A_{23} y'z' + 2A_{31} z'x' + 2A_{12} x'y' = 1 \quad (22)$$

The coefficients of the optical index ellipsoid in the transformed system may be written in terms of the coefficients of the optical index ellipsoid in the original coordinate system. Using Eq. (16),



one may write,

$$\begin{aligned}
 A_{11} &= B_{11}\ell_1^2 + B_{22}\ell_2^2 + B_{33}\ell_3^2 + 2(B_{23}\ell_2\ell_3 + B_{31}\ell_3\ell_1 + B_{12}\ell_1\ell_2) \\
 \text{-----} & \\
 A_{12} &= B_{11}\ell_1 m_1 + B_{22}\ell_2 m_2 + B_{33}\ell_3 m_3 + B_{23}(\ell_2 m_3 + \ell_3 m_2) + B_{31}(\ell_3 m_1 + \ell_1 m_3) \\
 &\quad + B_{12}(\ell_1 m_2 + \ell_2 m_1)
 \end{aligned} \tag{23}$$

Combining Eqs. (17) and (23),

$$\begin{aligned}
 A_{11} &= B_{11} & A_{23} &= -\frac{1}{2} B_{22} + \frac{1}{2} B_{33} \\
 A_{22} &= \frac{1}{2} B_{22} + \frac{1}{2} B_{33} + B_{23} & A_{31} &= \frac{1}{\sqrt{2}} B_{31} - \frac{1}{\sqrt{2}} B_{12} \\
 A_{33} &= \frac{1}{2} B_{22} + \frac{1}{2} B_{33} - B_{23} & A_{12} &= \frac{1}{\sqrt{2}} B_{31} + \frac{1}{\sqrt{2}} B_{12}
 \end{aligned} \tag{24}$$

For observation along the Y' axis, the cross section of the index ellipsoid is, in general,

$$A_{11} x'^2 + A_{33} z'^2 + 2 A_{31} z'x' = 1 \tag{25}$$

The values of  $A_{11}$ ,  $A_{33}$ , and  $A_{31}$  may be determined from Eqs. (21)

and (24):

$$\begin{aligned}
 A_{11} &= p_{11} S'_{11} + B_{11}^0 \\
 A_{33} &= \frac{1}{2} (p_{12} + p_{31} + p_{41}) S'_{11} + \frac{1}{2} (B_{22}^0 + B_{33}^0) \\
 A_{31} &= 0
 \end{aligned} \tag{26}$$

Note that  $A_{31} = 0$ , indicating in this particular case, that the ellipse is not tilted with respect to the new coordinate axes.

In general, for a rotated system with respect to the crystallographic axes, the procedure is: 1. Write the strains in the unprimed system in terms of the strains in the primed system. 2. Write the difference of coefficients of the index ellipsoid in the unprimed system in terms of the strains in the primed system.

3. Write the coefficients of the index ellipsoid in the primed system in terms of the coefficients in the unprimed system. Briefly then, one wants to write the photoelastic constants, as originally defined in a rectangular coordinate system, in the coordinate system in which the investigation is being carried out, which in general, is rotated with respect to the system defined by the crystallographic axes.

SECTION C: Dynamic measurements: Introduction of a strain in a transparent medium results in a change in the index of refraction of the medium. The optical parameters discussed earlier are the indices of refraction for a crystal. Thus, the lengths of the axes of the index ellipsoid are proportional to the indices of refraction of the medium and are also proportional to the pressure or strain exerted on the medium. In the case of an ultrasonic wave providing the strain, the axes of the index ellipsoid will vary periodically, where the periodicity is determined by the frequency of the ultrasonic wave.

Consider the two cases discussed earlier; in Case 1, repeating Eq. (15):

$$\begin{aligned} B_{11} - B_{11}^0 &= p_{13} S_{33} = \frac{1}{n_{11}'^2} - \frac{1}{n_{11}^2} \\ B_{33} - B_{33}^0 &= p_{33} S_{33} = \frac{1}{n_{33}'^2} - \frac{1}{n_{33}^2} \end{aligned} \quad (15)$$

$B_{31} - 0 = 0$ , indicating no tilt of the index ellipse.

Since  $S_{33}$  is a periodic strain, the axes of the index ellipse vary periodically. Following Mueller (2),  $B_{11}$  and  $B_{33}$  may be written as:



$$B_{11} = \frac{1}{n_{11}^2} - i_1 (2\pi f^* A k \sqrt{\rho} \sin 2\pi f^*(t - (z \cos \varnothing + y \sin \varnothing)/V^*)) \quad (27)$$

$$B_{33} = \frac{1}{n_{33}^2} - i_3 (2\pi f^* A k \sqrt{\rho} \sin 2\pi f^*(t - (z \cos \varnothing + y \sin \varnothing)/V^*))$$

where  $f^*$  = sound frequency

$\rho$  = density of the medium

$V^*$  = sound velocity

$A$  = amplitude of the sound waves

$k$  = constant proportional to the elastic constants of the medium.

This indicates that  $i_1$  and  $i_3$  are proportional to the amplitude of variation of the principle axes of the index ellipsoid. From the above equations, one obtains:

$$\frac{i_1}{i_3} = \frac{B_{11} - 1/n_{11}^2}{B_{33} - 1/n_{33}^2} = \frac{p_{13} s_{33}}{p_{33} s_{33}} = \frac{p_{13}}{p_{33}}$$

Let  $\Delta n_{11}$  and  $\Delta n_{33}$  be the change in the index of refraction along the X and Z directions respectively. One may then write:

$$B_{11} = \frac{1}{(n_{11} + \Delta n_{11})^2} = \frac{1}{(1 + \Delta n_{11}/n_{11})^2 n_{11}^2} = \frac{1 - 2\Delta n_{11}/n_{11}}{n_{11}^2} = \frac{1}{n_{11}^2} - \frac{2\Delta n_{11}}{n_{11}^3} \quad (29)$$

$$B_{33} = \frac{1}{(n_{33} + \Delta n_{33})^2} = \frac{1}{(1 + \Delta n_{33}/n_{33})^2 n_{33}^2} = \frac{1 - 2\Delta n_{33}/n_{33}}{n_{33}^2} = \frac{1}{n_{33}^2} - \frac{2\Delta n_{33}}{n_{33}^3}$$

Comparing again with Mueller's equations;

$$(i_1)(K)(n_{11})^3 = \Delta n_{11} \quad \text{and} \quad (i_1)(K)(n_{33})^3 = \Delta n_{33}$$

Therefore,

$$\frac{\Delta n_{11}}{\Delta n_{33}} = \frac{i_1 n_{11}^3}{i_3 n_{33}^3} = \frac{n_{11}^3 p_{13}}{n_{33}^3 p_{33}} = \frac{n_o^3 p_{13}}{n_e^3 p_{33}} = R_1 \quad (30)$$

From the theory of Raman and Nath (5), one may show that a change in both  $n_{11}$  and  $n_{33}$  produces two diffraction patterns and the intensity of each pattern is dependent upon  $\Delta n_{11}$  and  $\Delta n_{33}$  respectively. Thus, if the  $m^{\text{th}}$  order of the diffraction pattern due to  $\Delta n_{11}$  is observed, the amplitude will be

$$E_{m1} = E_1 J_m(v_1),$$

where  $E_1$  is the magnitude of the electric vector of the incident light. Similarly for the pattern due to  $\Delta n_{33}$ ,

$$E_{m3} = E_3 J_m(v_3)$$

where

$$v_1 = \frac{2\pi \Delta n_{11} L}{\lambda} \quad v_3 = \frac{2\pi \Delta n_{33} L}{\lambda}$$

$J_m$  is the  $m^{\text{th}}$  order Bessel Function,  $L$  is the width of the sound field, and  $\lambda$  is the wavelength of the light. For small values of  $m$  and  $v$ ,

$$\frac{E_{m1}}{E_{m3}} = \frac{E_1(v_1)^m}{E_3(v_3)^m} = \frac{E_1}{E_3} \left( \frac{\Delta n_{11}}{\Delta n_{33}} \right)^m = R_1^m \quad (31)$$

If the light is polarized at  $45^\circ$  to the sound field,  $E_1 = E_3$  and

$$R_1^m = \frac{n_o^3}{n_e^3} \frac{p_{13}}{p_{33}} \quad (32)$$

where  $R_1^m$  is the quantity that is experimentally determined. In this investigation, only the intensity in the first order diffraction pattern was measured, therefore,  $m = 1$ . For Case 2, following the same procedure, one obtains:

$$\begin{aligned} A_{11} - 1/n_{11}^2 &= p_{11} S_{11}' \\ A_{33} - 1/n_{33}^2 &= \frac{1}{2} (p_{12} + p_{31} - 2 p_{41}) S_{11}' \end{aligned} \quad (26)$$

From Eq. (28), where the system is rotated, so that  $A_{11}$  and  $A_{33}$  are used instead of  $B_{11}$  and  $B_{33}$ , the ratio can be written as

$$\frac{i_3}{i_1} = \frac{A_{33} - 1/n_{33}^2}{A_{11} - 1/n_{11}^2} = \frac{(p_{12} + p_{31} - 2 p_{41}) S_{11}'}{2 p_{11} S_{11}'} = \frac{n_{33}^3 (p_{12} + p_{31} - 2 p_{41})}{n_{11}^2 (2 p_{11})} = R_1^m \quad (33)$$

where the ratio  $R_1^m$  is the experimentally determined quantity.

**SECTION D: Static Measurements:** By applying a static or constant stress to the sapphire crystal and measuring the relative change in optical path length with a Babinet Compensator, a relationship involving differences of photoelastic constants is obtained. To illustrate, following Vedam (10) assume a crystal whose dimensions are oriented along the orthogonal set of axes has a strain (stress) in the X direction and observation is in the Z direction. From Eq. (11)

$$\begin{aligned} B_{11} - B_{11}^0 &= p_{11} S_{11} \\ B_{22} - B_{22}^0 &= p_{12} S_{11} \\ B_{33} - B_{33}^0 &= p_{31} S_{11} \\ B_{23} &= p_{41} S_{11} \end{aligned} \quad (34)$$

Since  $B_{11}^0 = 1/n_{11}^2$ ,  $\Delta B_{11}^0 = - \frac{2\Delta n_{11}}{n_{11}^3}$

but  $B_{11} - B_{11}^0$  is equal to  $\Delta B_{11}^0$ , thus,

$$B_{11} - B_{11}^0 = \Delta B_{11}^0 = - \frac{2\Delta n_{11}}{n_{11}^3} = p_{11} S_{11} \quad (35)$$

or, rearranging,

$$\Delta n_{11} = \frac{-n_{11}^3 p_{11} S_{11}}{2} \quad (36)$$

The differential path retardation is obtained from  $\Delta(n_{11}z)$  where  $z$  is the distance the light travels in the sample, and  $(n_{11}z)$  is defined as the optical path length.

$$\Delta(n_{11}z) = (\Delta n_{11})(z) + (n_{11})(\Delta z) = \delta_{11} \quad (37)$$

Note that  $\Delta n_{11}$  has been defined above and  $\Delta z$  is the strain in the  $z$  direction, i.e.,  $S_{33}$ . Rewriting Eq. (33) and using Eqs. (32) and (8), one obtains

$$\delta_{11} = \Delta n_{11} z + n_{11} \Delta z = - \frac{n_{11}^3 p_{11} S_{11} z}{2} - n_{11} z S_{13} T_{11} \quad (38)$$

The same procedure may be carried through for  $\delta_{22}$ , corresponding to  $n_{22}$ , with the result that,

$$\delta_{22} = - \frac{n_{22}^3 p_{12} S_{11} z}{2} - n_{22} S_{13} z T_{11} \quad (39)$$

The relative retardation is defined as the difference of equations (35) and (34) and this retardation is equal to the phase difference of the two beams of light, i.e.,

$$B \cdot 2\pi = \frac{2\pi}{\lambda} (\delta_{11} - \delta_{22}) \quad (40)$$





where  $B$  is some fraction of  $2\pi$  which determines how much phase change occurs, and  $\lambda$  is the wavelength of the light. Rewriting Eq. (36), using the values of  $\delta_{11}$  and  $\delta_{22}$  from Eqs. (34) and (35),

$$B = \frac{1}{\lambda} \left[ \frac{-n_{11}^3 p_{11} s_{11} z}{2} - n_{11} z s_{13} T_{11} \right] - \frac{1}{\lambda} \left[ \frac{-n_{22}^3 p_{12} s_{11} z}{2} - n_{22} s_{13} z T_{11} \right]$$

$$B = \frac{z}{\lambda} \left[ \frac{(n_{22}^3 p_{12} - n_{11}^3 p_{11}) s_{11}}{2} + s_{13} T_{11} (n_{22} - n_{11}) \right] \quad (41)$$

but  $n_{11}$  and  $n_{22}$ , which correspond to the  $n_o$  of the crystal, are equal, so Eq. (37) may be written as

$$B = \frac{z}{\lambda} \frac{n_o^3}{2} s_{11} (p_{12} - p_{11}) \quad (42)$$

Assuming uniform stress throughout the medium of the specimen,  $S_{11}$  may be written as

$$S_{11} = s_{11} T_{11} \quad (43)$$

where  $s_{11}$  is the elastic modulus. Also,  $T_{11} = F/A$

where  $F$  is the force on the specimen and  $A$  is the area over which the force is applied. Finally then,

$$p_{12} - p_{11} = \frac{2B \lambda A}{d n_{11}^3 F S_{11}} \quad (44)$$

Table I provides a complete list of observation directions, strain directions, and the relationships of photoelastic constants for those directions which are used in this investigation. The direction cosines of the normals to the cube faces with respect to an orthogonal set of axes are given to indicate the orientation of the cubes used.

TABLE I

<u>Crystal Number 1:</u>	
$(1,0,0); (0,1,0); (0,0,1)$	
<u>Sound</u>	<u>Light</u>
x-axis	z-axis
x-axis	y-axis
z-axis	x-axis
<u>Strain</u>	<u>Relationship</u>
x-axis	$p_{12}/p_{11}$
z-axis	$p_{31}/p_{11}$
	$p_{13}/p_{33}$
<u>Crystal Number 2:</u>	
$(1,0,0); (0, \frac{1}{2}, \frac{1}{2}); (0, -\frac{1}{2}, \frac{1}{2})$	
<u>Sound</u>	<u>Relationship</u>
x'-axis	$(p_{12} + p_{31} - 2p_{41})/2p_{11}$
x'-axis	$(p_{12} + p_{31} + 2p_{41})/2p_{11}$

Crystal Number 3:

(1,0,0) ; (0,.620,.784); (0,.775,-.632)

TABLE I (continued)

<u>Sound</u>	<u>Light</u>		<u>Relationship</u>
x'-axis	y'-axis	$\frac{I_z'}{I_x'}$ =	$\frac{.608 p_{12} + .392 p_{31} + .976 p_{41}}{p_{11}}$
x'-axis	z'-axis	$\frac{I_y'}{I_x'}$ =	$\frac{.608 p_{12} + .392 p_{31} + .976 p_{41}}{p_{11}}$
y'-axis	z'-axis	$\frac{I_x'}{I_y'}$ =	$\frac{.392 p_{12} + .608 p_{13} + .488 p_{14}}{.154 p_{11} + .238 p_{13} + .191 p_{14} + .238 p_{31} + .370 p_{33} + .476 p_{44} + .383 p_{41}}$
y'-axis	x'-axis	$\frac{I_z'}{I_y'}$ =	$\frac{.238 p_{11} + .370 p_{13} + .297 p_{14} + .154 p_{31} + .238 p_{33} + .383 p_{41} + .476 p_{44}}{.154 p_{11} + .238 p_{13} + .191 p_{14} + .238 p_{31} + .370 p_{33} + .383 p_{41} + .476 p_{44}}$
z'-axis	y'-axis	$\frac{I_x'}{I_z'}$ =	$\frac{.608 p_{12} + .392 p_{13} + .488 p_{14}}{.370 p_{11} + .238 p_{13} + .297 p_{14} + .238 p_{31} + .154 p_{33} + .593 p_{41} + .476 p_{44}}$
z'-axis	x'-axis	$\frac{I_y'}{I_z'}$ =	$\frac{.238 p_{11} + .154 p_{13} + .191 p_{14} + .370 p_{31} + .238 p_{33} + .593 p_{41} + .476 p_{44}}{.370 p_{11} + .238 p_{13} + .297 p_{14} + .238 p_{31} + .154 p_{33} + .593 p_{41} + .476 p_{44}}$

.....

.....

.....

.....

.....

.....

.....

.....

.....

.....

.....

.....

.....

.....

.....

.....

.....

.....

.....

.....

.....

.....

.....

.....

.....

.....

.....

.....

.....

.....

.....

.....

.....

.....

.....

.....

.....

.....

.....

.....

.....

.....

.....

.....

.....

.....

.....

.....

.....

.....

.....

.....

.....

.....

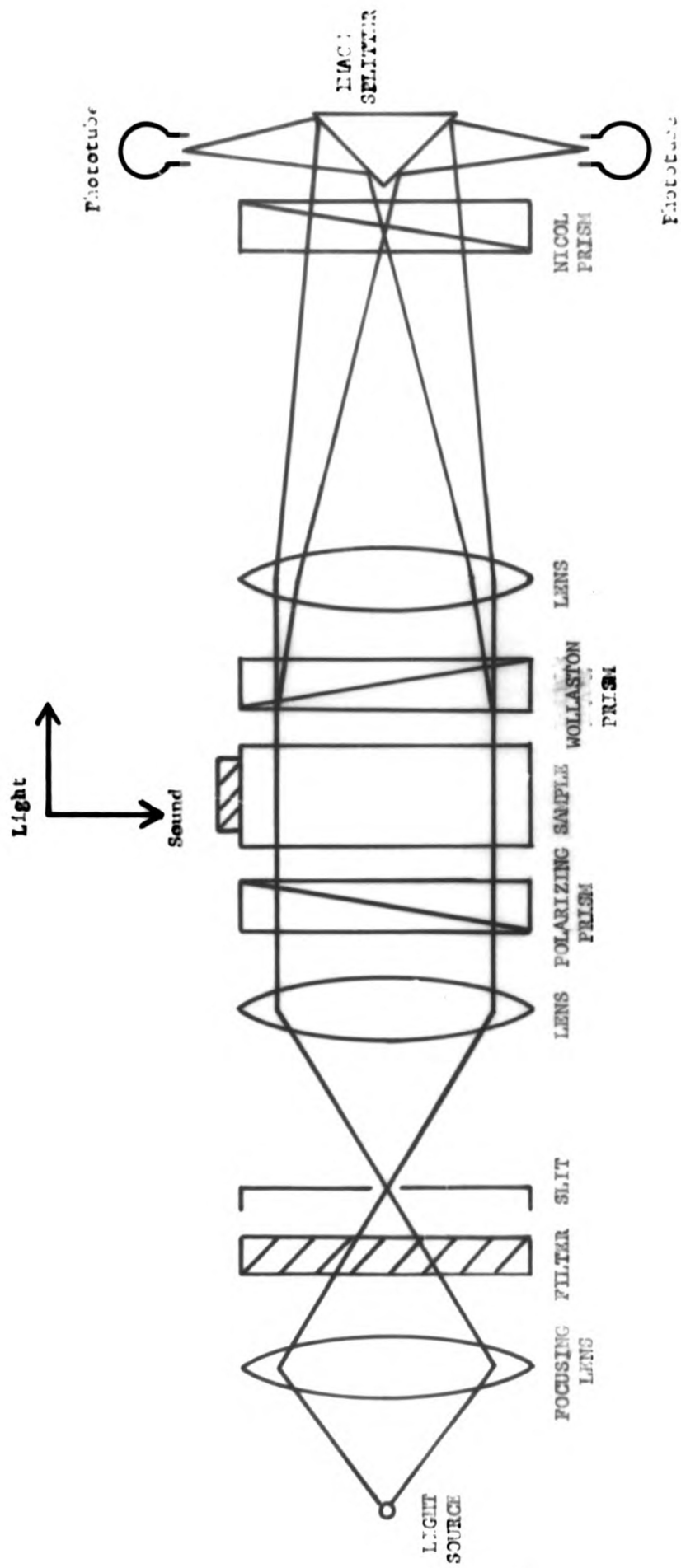
.....

.....

.....

## EXPERIMENTAL PROCEDURE

Dynamic Measurements: See Fig. 4. The experimental apparatus consisted of a mercury arc light source filtered to obtain the 5461 Å green line of mercury. The light was focused on a vertical slit which acted as an image for the measurements. Light from the slit was collimated and passed through a Nicol polarizing prism, which polarized the light at  $45^{\circ}$  to the vertical. The light then passed through the sample perpendicular to the path of the sound. The Wollaston double image prism splits the light into two rays, one polarized in a direction parallel to the sound beam and the other polarized perpendicular to the sound beam. The light then passed through a focusing lens and analyzing prism, after which the two rays were split by a right angle mirror, each ray going to a pick-up tube of a differential photometer. The pick-up tubes of the differential photomultiplier were adjusted so that their slits were in the focal plane of the focusing lens. The sound source is an X-cut 10 megacycle quartz crystal, driven by a continuous wave, variable frequency oscillator. Standing sound waves are produced in the sapphire sample by the quartz crystal. These standing waves produce a diffraction pattern of the slit image in the focal plane of the focusing lens. If the investigations are carried out at low sound intensities, it can be assumed that light in the first order diffraction pattern created by the standing sound waves is plane polarized, but rotated at an angle with respect to its original direction



EXPERIMENTAL APPARATUS

FIGURE 1.



of polarization. If the sound is a pure longitudinal wave, and the incident light is polarized at  $45^\circ$  to the vertical, then from Mueller (2), one may write,

$$\tan (\alpha + 45^\circ) = \frac{J_m (R_1 v_1)}{J_m (v_1)} \approx R_1^m \quad (45)$$

for low  $v$  and  $m$ . See Eq. (31).

$\alpha$  is the angle of rotation of the plane polarized light,

$R_1 v_1$  is the Raman-Nath parameter for light polarized perpendicular to the sound beam, and  $v_1$  is the Raman-Nath parameter for light polarized parallel to the sound beam. Mueller suggested three methods of measuring photoelastic constants. Method "C" utilizes a double image prism, which separates the light into two components, one polarized parallel to the sound beam and the other polarized perpendicular to the sound beam, which is exactly the procedure used in this investigation.

The experimental procedure used in taking measurements is to adjust the analyzing prism so that each phototube is subject to equal intensity of light, i.e., at  $45^\circ$  to the vertical. The phototubes were adjusted to allow only the first order diffraction pattern to pass through their slits. The sound is then turned on and the analyzing prism rotated until the first orders were of equal intensity. With the differential photometer, this would correspond to a null or minimum reading. If the angle of rotation to equalize the intensities of the first order diffraction line is  $\alpha$ , then  $\tan (45^\circ + \alpha)$  is the  $R_1$  of



Eq. (45).

Static Measurements: See Fig. 5. The same light source and filtering arrangement is used here as was used in the dynamic measurements. Collimated light is polarized at  $45^\circ$  to the vertical and is incident normal to the specimen. Light then passes through the Babinet Compensator and an analyzing Nicol prism set in the crossed position with respect to the polarizing prism. The fringe system produced by the Babinet Compensator is viewed at the focal plane of the focusing lens with an eyepiece. The specimen is uniformly stressed with an apparatus similar to that used by Waxler and Napolitano (11). See Figs. 6. The Babinet Compensator has a calibrated movement and the experimental procedure is to find the number of divisions  $N$  for a phase change of  $2\pi$ , which is a constant for the instrument. After applying a known load to the specimen, a fringe shift occurs. The fringe is then reset to its initial position by movement through  $n$  divisions of the Babinet Compensator. This ratio of  $n$  divisions for a given load to  $N$  divisions for a phase change of  $2\pi$  is the experimentally determined  $B$ , used in Eq. (40).

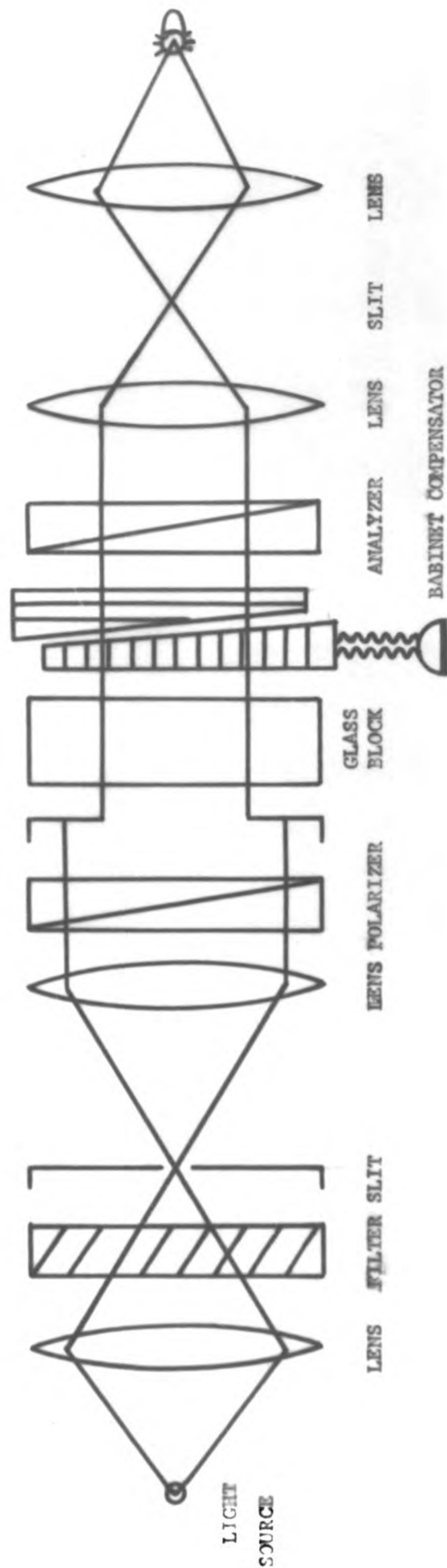
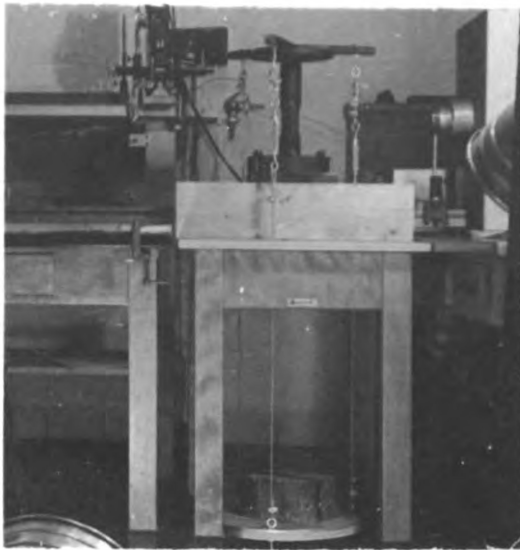
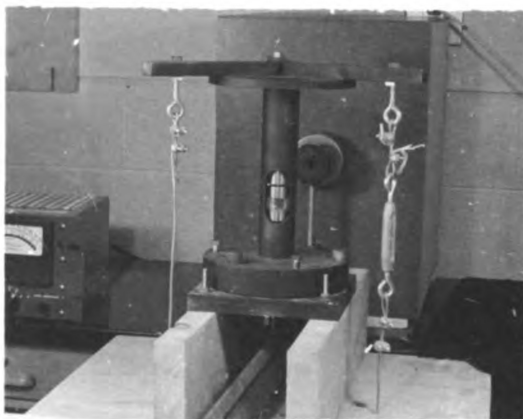


FIGURE 5.

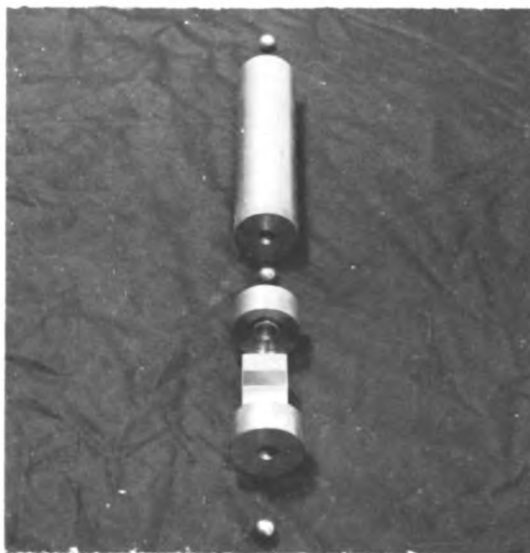
FIGURE 6.



Side view of stressing table.



End view of stressing table, showing  
sapphire cube position when under stress.



Exploded view of piston-type pressure transmitter.



# EXPERIMENTAL RESULTS

Ratio: $p_{12}/p_{11}$		Ratio: $p_{31}/p_{11}$	
<u>(Voltage)<sup>2</sup></u>	<u>Tan(<math>\alpha + 45^\circ</math>)</u>	<u>(Voltage)<sup>2</sup></u>	<u>Tan(<math>\alpha + 45^\circ</math>)</u>
$2.25 \times 10^4 (v.)^2$	3.25	$9.00 \times 10^4 (v.)^2$	5.14
4.00	3.19	12.25	4.92
6.25	3.01	16.00	4.83
9.00	2.92	18.06	4.55
12.25	2.90		
16.00	2.72		

Ratio: $(p_{12} + p_{31} + 2p_{41})/2p_{11}$		Ratio: $p_{13}/p_{33}$	
<u>(Voltage)<sup>2</sup></u>	<u>Tan(<math>\alpha + 45^\circ</math>)</u>	<u>(Voltage)<sup>2</sup></u>	<u>Tan(<math>\alpha + 45^\circ</math>)</u>
$2.25 \times 10^4 (v.)^2$	4.20	$6.25 \times 10^4 (v.)^2$	6.94
4.00	4.17	9.00	6.61
6.25	3.98	12.25	6.31
9.00	3.78	16.00	5.67
12.25	3.58	20.25	5.10
16.00	3.27		

Ratio: $I_x/I_y$		Ratio: $I_x/I_z$	
<u>(Voltage)<sup>2</sup></u>	<u>Tan(<math>\alpha + 45^\circ</math>)</u>	<u>(Voltage)<sup>2</sup></u>	<u>Tan(<math>\alpha + 45^\circ</math>)</u>
$4.00 \times 10^4 (v.)^2$	2.45	$2.25 \times 10^4 (v.)^2$	1.81
6.25	2.38	4.00	1.67
9.00	2.31	6.25	1.52
12.25	2.26	9.00	1.45
16.00	2.20	12.25	1.37
		16.00	1.31

Determination of  $N$  (= phase change of  $2\pi$ ) for the Babinet Compensator: Sixty measurements were made to obtain the number of divisions on the drumhead of Babinet Compensator corresponding to a phase change of  $2\pi$  between the ordinary and extraordinary ray.  $N$  for the Babinet Compensator used is 1288 divisions. Below are the tabulated values of  $n/kg.$  for the determination of  $p_{11} - p_{12}$  and  $p_{13} - p_{33}$ :

<u><math>p_{12} - p_{11}</math></u>	<u><math>n/kg.</math></u>	<u><math>n/kg.</math></u>	<u><math>n/kg.</math></u>	<u><math>n/kg.</math></u>
	5.93	2.89	3.85	4.43
	4.76	4.73	4.18	3.74
	3.92	4.58	4.84	6.48
	5.60	5.20	6.15	4.62
	4.43	4.14	3.85	3.66
	5.53	4.21	4.54	5.57
	5.38	5.09	5.24	4.58
	3.66	4.18	4.25	3.70
	3.66	4.07	4.58	4.36
	3.81	4.18	6.56	6.52

$$n_{av}/kg. = 4.64$$

<u><math>p_{13} - p_{33}</math></u>	<u><math>n/kg.</math></u>	<u><math>n/kg.</math></u>	<u><math>n/kg.</math></u>	<u><math>n/kg.</math></u>
	2.42	1.87	2.67	2.53
	2.53	2.31	2.45	1.94
	2.31	2.31	2.49	2.09
	2.34	1.94	1.43	2.27
	2.93	2.09	2.45	2.75
	2.93	2.56	3.04	3.59
	2.56	1.54	2.82	3.11
	2.53	1.32	1.79	1.65
	1.90	2.20	2.64	2.86
	2.45	1.50	2.12	2.82

$$n_{av}/kg. = 2.31$$



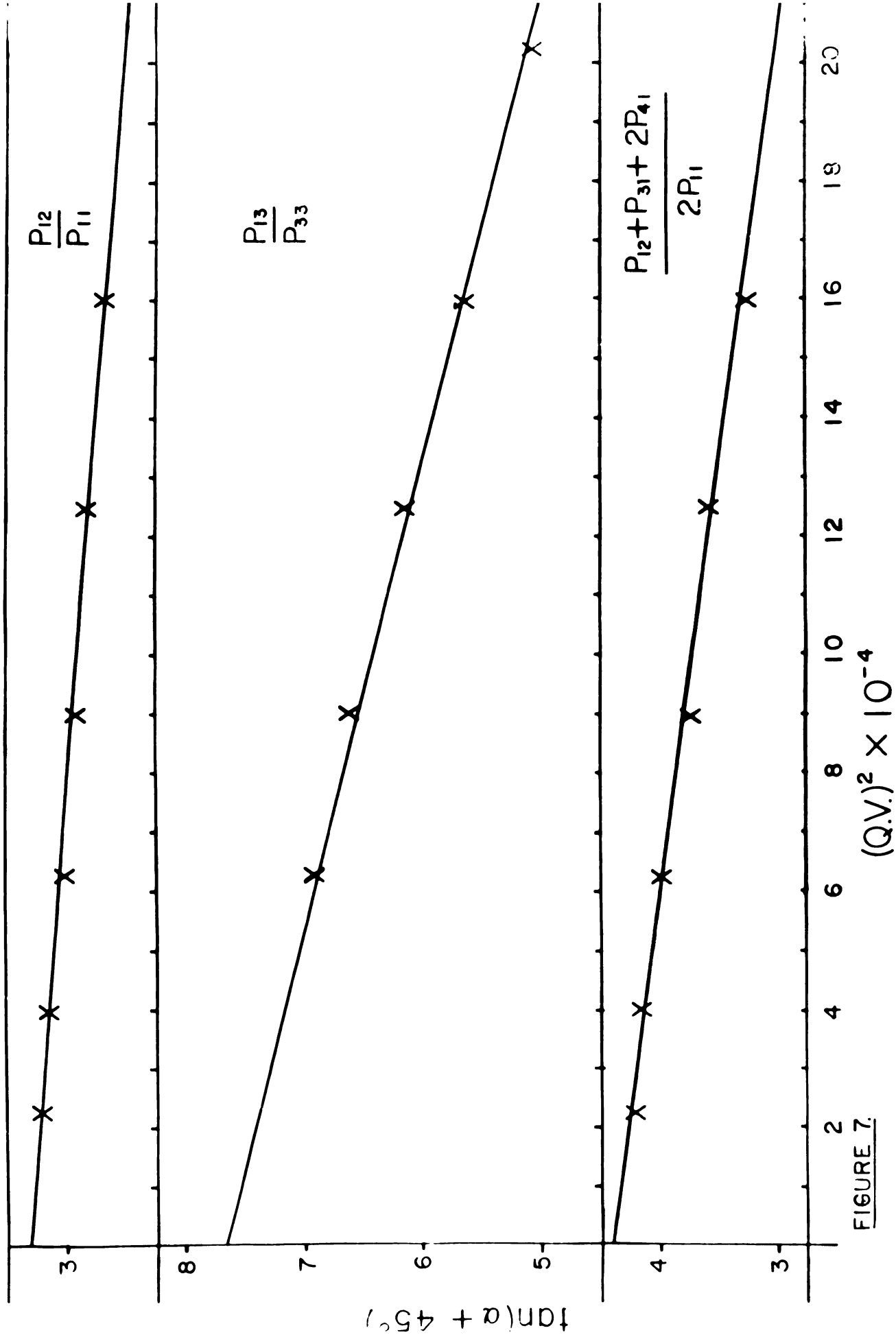


FIGURE 7.



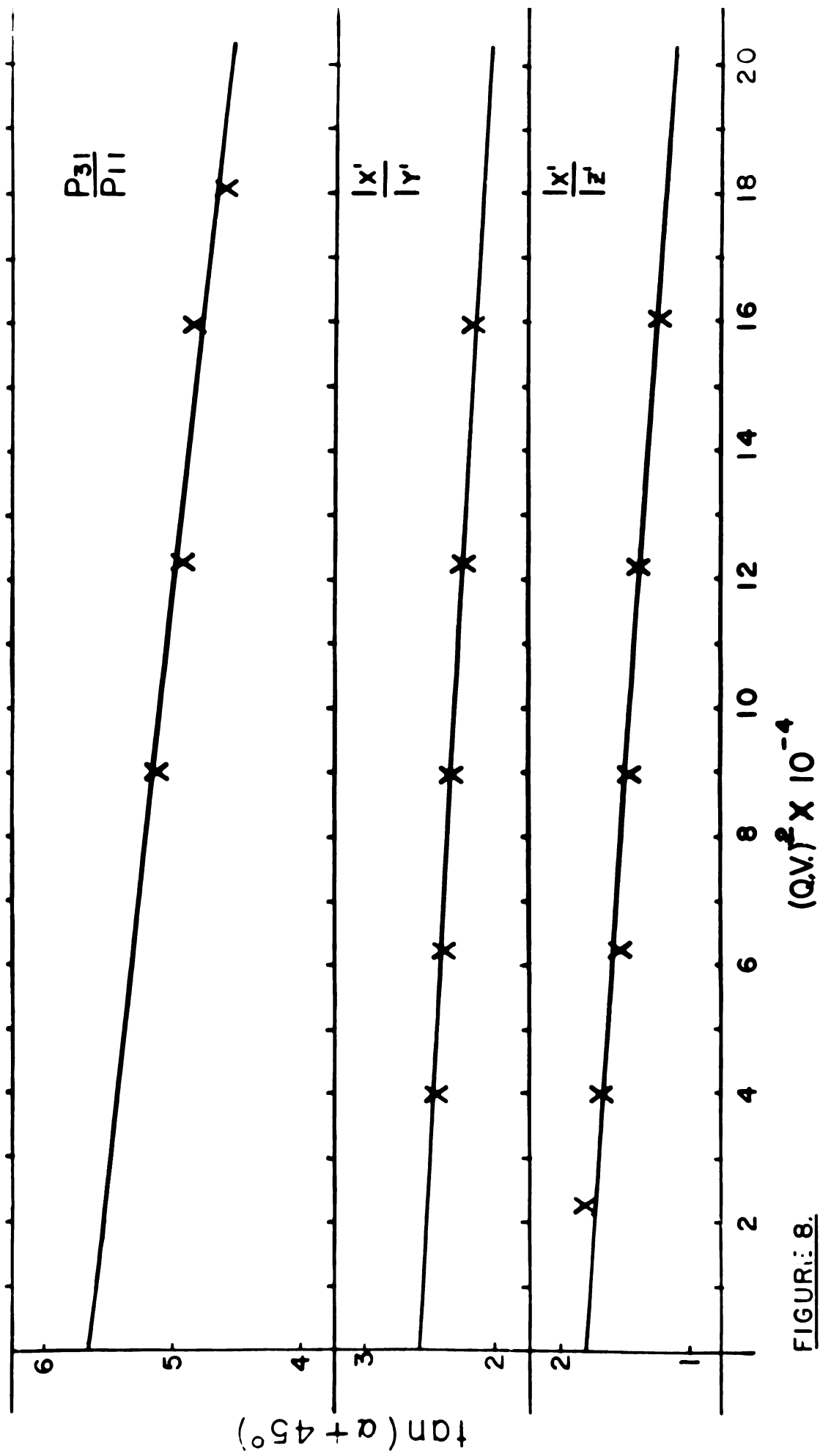


FIGURE 8.

Sample calculation of Photoelastic Constants:

Repeating Eq. (44), one may write,

$$P_{12} - P_{11} = \frac{2 n A}{N d n_o^3 W g S_{11}}$$

where,

$$n/W = 4.64 \text{ div./kg.}$$

$$N = 1288 \text{ div.}$$

$$= 5.461 \times 10^{-5} \text{ cm.}$$

$$n_o = 1.771 \quad (\text{Reference (12)})$$

$$n_o^3 = 5.554$$

$$A = (1.60)^2 \text{ cm}^2.$$

$$d = 1.60 \text{ cm.}$$

$$g = 980 \text{ cm./sec.}^2$$

$$S_{11} = 2.28 \times 10^{-13} \text{ cm}^2/\text{dyne} \quad (\text{Reference (8)})$$

$$P_{12} - P_{11} = \frac{(4.64)(5.461)(10^{-5})(2)(1.60)^2}{(10)^3(1.288)(1.60)(5.554)(9.8)(10)^2(2.28)(10)^{-13}}$$

$$P_{12} - P_{11} = \frac{(\text{cm.})(\text{cm})^2}{\frac{(\text{gms})(\text{cm})(\text{cm})(\text{cm})^2}{(\text{sec})^2(\text{gm})(\text{cm})}} = (\text{unitless})$$

$$P_{12} - P_{11} = 0.507$$

$$P_{12}/P_{11} = +3.31 \quad (\text{From dynamic measurements. See Fig. 7})$$

The determination of the sign of the ratio of photoelastic constants follows the convention suggested by Hagelberg (13).

Combination of the two equations yields,

$$P_{11} = 0.219$$

$$P_{12} = 0.725$$

Table II. Strain optical constants of synthetic sapphire.

$$p_{11} = 0.219$$

$$p_{12} = 0.725$$

$$p_{13} = 0.311$$

$$p_{14} = -0.029$$

$$p_{31} = 1.259$$

$$p_{33} = 0.041$$

$$p_{41} = 0.119$$

$$p_{44} = -0.418$$

Table III. Stress optical constants of synthetic sapphire.

$$q_{11} = -0.037$$

$$q_{12} = 1.396$$

$$q_{13} = 2.163$$

$$q_{14} = 0.014$$

$$q_{31} = 0.300$$

$$q_{33} = -0.539$$

$$q_{41} = 0.225$$

$$q_{44} = -2.916$$

In units of  $10^{-13} \text{ cm}^2/\text{dyne}$

## BIBLIOGRAPHY

1. E. G. Coker and L. N. G. Filon, "Photoelasticity" Cambridge University Press. London, 1957.
2. H. Mueller, Z. Krist. A99, 122 (1938).
3. H. Mueller, Phys. Rev. 52, 223 (1937).
4. H. Mueller, Phys. Rev. 47, 948 (1935).
5. C. V. Raman and N. S. N. Nath, Proc. Ind. Acad. Sci. A2, 406 (1935).
6. T. S. Narasimhamurty, Acta Cryst. 14, 1176 (1961).
7. F. E. Borgnis, Phys. Rev. 98, 1000 (1955).
8. W. G. Mayer and E. A. Hiedemann, J. Acoust. Soc. Am. 32, 1699 (1960).
9. T. S. Narasimhamurty, "Photoelasticity of Crystals and Glasses" Publication at M. S. U., 1960.
10. K. Vedam, Ind. Acad. Sci. (Proc.) A34, 161 (1951).
11. R. M. Waxler and A. Napolitano, J. Research. Natl. Bur. Standards. 59, 121 (1957).
12. M. A. Jeppeson, J. Opt. Soc. Am. 48, 629 (1958).
13. M. P. Hagelberg, "The Diffraction of Linearly Polarized Light by Ultrasonic Waves in Transparent Solids" Ph.D. Thesis. M. S. U., 1961.
14. W. G. Cady, "Piezoelectricity" McGraw-Hill Book Company. New York, 1946.

MICHIGAN STATE UNIV. LIBRARIES



31293017040043